# Cyclin-dependent kinase 4 drives cystic kidney disease in the absence of mTORC1 signaling activity

Check for updates

OPEN

Florian Grahammer[1,2,21], Bernhard Dumoulin[1,2,21], Ramila E. Gulieva[3,4,5,6], Hui Wu[1,2], Yaoxian Xu[7], Nurgazy Sulaimanov[8], Frederic Arnold[9], Lukas Sandner[9], Tomke Cordts[9], Abhijeet Todkar[9], Pierre Moulin[10], Wilfried Reichardt[11], Victor G. Puelles[1,2,12,13], Rafael Kramann[7,14,15], Benjamin S. Freedman[3,4,5,6,16], Hauke Busch[17,21], Melanie Boerries[18,19,21], Gerd Walz[9,20,21] and Tobias B. Huber[1,2,21]

*[1]III. Department of Medicine, University Hospital Hamburg Eppendorf, Hamburg, Germany; [2]Hamburg Center for Kidney Health (HCKH), University Medical Center Hamburg-Eppendorf, Hamburg, Germany; [3]Division of Nephrology, University of Washington School of Medicine, Seattle, Washington, USA; [4]Kidney Research Institute, University of Washington School of Medicine, Seattle, Washington, USA; [5]Institute for Stem Cell and Regenerative Medicine, University of Washington School of Medicine, Seattle, Washington, USA; [6]Department of Medicine, University of Washington School of Medicine, Seattle, Washington, USA; [7]Institute of Experimental Medicine and Systems Biology, Medical Faculty, Rheinisch-Westfälische Technische Hochschule (RWTH) Aachen University, Aachen, Germany; [8]Department of Electrical Engineering and Information Technology, Technische Universität Darmstadt, Darmstadt, Germany; [9]Department of Medicine IV, Medical Center and Faculty of Medicine University of Freiburg, Freiburg, Germany; [10]Institute of Pathology, Centre Hospitalier Universitaire Vaudois, Lausanne University, Lausanne, Switzerland; [11]Department of Diagnostic and Interventional Radiology, Division of Medical Physics, University Medical Center Freiburg, Faculty of Medicine, University of Freiburg, Freiburg, Germany; [12]Department of Clinical Medicine, Aarhus University, Aarhus, Denmark; [13]Department of Pathology, Aarhus University Hospital, Aarhus, Denmark; [14]Division of Nephrology and Clinical Immunology, Rheinisch-Westfälische Technische Hochschule (RWTH) Aachen University, Aachen, Germany; [15]Department of Internal Medicine, Nephrology and Transplantation, Erasmus Medical Center, Rotterdam, the Netherlands; [16]Plurexa LLC, Seattle, Washington, USA; [17]Lübeck Institute of Experimental Dermatology, University of Lübeck, Lübeck, Germany; [18]Institute of Medical Bioinformatics and Systems Medicine, Medical Center and Faculty of Medicine University of Freiburg, Freiburg, Germany; [19]German Cancer Consortium (DKTK), Partner site Freiburg, a partnership between Deutsches Krebs Forschungs Zentrum (DKFZ) and Medical Center–University of Freiburg, Heidelberg, Germany; and [20]Signaling Research Centres BIOSS and CIBSS, University of Freiburg, Freiburg, Germany*

**Progression of cystic kidney disease has been linked to activation of the mTORC1 signaling pathway. Yet the utility of mTORC1 inhibitors to treat patients with polycystic kidney disease remains controversial despite promising preclinical data. To define the cell intrinsic role of mTORC1 for cyst development, the mTORC1 subunit gene *Raptor* was selectively inactivated in kidney tubular cells lacking cilia due to simultaneous deletion of the kinesin family member gene *Kif3A*. In contrast to a rapid onset of cyst formation and kidney failure in mice with defective ciliogenesis, both kidney function, cyst formation discerned by magnetic resonance imaging and overall survival were strikingly improved in mice additionally lacking *Raptor*. However, these mice eventually succumbed to cystic kidney disease despite mTORC1 inactivation. In-depth transcriptome analysis revealed the rapid activation of other growth-promoting signaling pathways, overriding the effects of mTORC1 deletion and identified cyclin-dependent kinase (CDK) 4 as an alternate driver of cyst growth. Additional inhibition of CDK4-dependent signaling by the CDK4/6 inhibitor Palbociclib markedly slowed disease progression in mice and human organoid models of polycystic kidney disease and potentiated the effects of mTORC1 deletion/inhibition. Our findings indicate that cystic kidneys rapidly adopt bypass mechanisms typically observed in drug resistant cancers. Thus, future clinical trials need to consider combinatorial or sequential therapies to improve therapeutic efficacy in patients with cystic kidney disease.**

*Kidney International* (2024) **106,** 856–869; https://doi.org/10.1016/j.kint.2024.08.021

KEYWORDS: bypass mechanism; CDK4; cystic kidney disease; mTOR pathway

Copyright © 2024, International Society of Nephrology. Published by Elsevier Inc. This is an open access article under the CC BY-NC-ND license (http://creativecommons.org/licenses/by-nc-nd/4.0/).

Polycystic kidney disease (PKD) is a heterogenic ciliopathy associated with the progressive destruction of the renal parenchyma and end-stage renal disease.[1] The most common ciliopathy is autosomal dominant PKD (ADPKD), caused by mutations of *PKD1* (coding for polycystin-1) or by mutations of *PKD2* (coding for polycystin-2/TRPP2 [transient receptor potential polycystic 2]).[2] Ciliopathies are caused by defective cilia and are almost universally associated with an increase in mammalian target

**Correspondence:** *Florian Grahammer, III. Department of Medicine, University Medical Center Hamburg-Eppendorf, Martinistrasse 52, 20246 Hamburg, Germany. E-mail: f.grahammer@uke.de*

[21]FG, BD, HB, MB, GW, and TBH contributed equally.

**Received 19 December 2022; revised 29 July 2024; accepted 2 August 2024; published online 31 August 2024**

## Translational Statement

Treatments to halt the progression of cystic kidney disease are scarce and only partially effective. Mammalian target of rapamycin complex 1 (mTORC1) has been implicated in driving cystic kidney disease, yet despite convincing preclinical data, its clinical utility remains controversial. In cystic mice, selective inactivation of mTORC1 in renal tubular cells improved kidney function and overall survival. However, cyst progression was only delayed but not halted. In-depth transcriptomic analysis identified mTORC2 as an alternate pathway for delayed cyst growth, with cyclin-dependent kinase 4 (CDK4) as the main driver. Subsequent inhibition of CDK4 with palbociclib markedly potentiated the effects of mTORC1 deletion. Similarly, CDK4 bypass and the benefit of synergistic inhibition of mTORC1 and CDK4/6 could be demonstrated in human organoid models of polycystic kidney disease. The rapid adaptation of cystic kidneys underscores the importance of evaluating sequential or combinatorial therapies in clinical trials.

of rapamycin complex 1 (mTORC1) activity.[3,4] Although the precise coupling between cilia and mTORC1 activation requires further clarification, the C-terminal domain of polycystin-1 interacts with the tuberous sclerosis complex to inhibit Ras homolog enriched in brain, a small GTPase and activator of mTORC1, suggesting that polycystin-1 can directly modulate mTORC1 activity.[5] Polycystin-1 mutations also result in mitogen-activated protein kinase and phosphatidylinositol-3′-kinase/AKT activation, leading to phosphorylation and inhibition of tuberous sclerosis complex.[6] In addition, flow activates ciliary liver kinase B1, resulting in adenosine monophosphate kinase activation and mTORC1 inhibition, providing another mechanism by which cilia can control mTORC1.[7]

mTORC1 facilitates growth, proliferation, and mitochondrial biogenesis of tubular epithelial cells.[8–11] Different mTORC1-specific inhibitors have been used to slow cyst growth in rodent models of cystic kidney disease. First demonstrated in the Han: SPRD rat model,[12] the beneficial effects of mTORC1 inhibition on cyst growth and kidney function were subsequently confirmed in several other murine models, including *orpk* (*Ift88*), *bpk* (*Bicc1*), and *Pkd1*-deficient mice.[5,13] However, placebo-controlled clinical trials failed to demonstrate a benefit in patients with ADPKD.[14,15] Thus, these trials question the role of mTORC1 as a cyst-promoting component and as a relevant therapeutic target in human disease. To clearly define the role of mTORC1 in cystic kidney disease and to reconcile the apparent discrepancies between preclinical and clinical outcomes, we generated mTORC1-deficient mice by deleting the essential mTORC1 subunit *Raptor* in renal tubular epithelial cells and triggered the development of renal cysts by simultaneously preventing ciliogenesis by eliminating *Kif3a*. Our results unambiguously demonstrate the crucial involvement of mTORC1 signaling in cyst formation and that the elimination of mTORC1 activity represents a powerful tool to inhibit disease progression. However, extensive gene profiling of mTORC1-deficient cystic mice also revealed that bypass signaling rapidly replaces mTORC1, highlighting the need for novel strategies to treat ADPKD.

## METHODS

### Animals

All animal experiments were conducted according to the *Guide for the Care and Use of Laboratory Animals* (National Institutes of Health), as well as the German law for the welfare of animals, and were approved by local governmental authorities (G-10/39, G-11/02). Mice were housed in a specific pathogen–free facility with free access to chow and water and a 12-hour day/night cycle. Breeding and genotyping were done according to standard procedures. All mice were on a C57Bl6/N background. *Raptor fl/fl* mice (generous gift by M. Hall and M.Ruegg, University Basel, Switzerland) have been described previously[16] and were crossed to *KspCre*[17] and *Kif3a fl/fl*[18] mice. Mice were derived from *Kif3a fl/+*Raptor fl/+*KspCre* and *Kif3a fl/+*Raptor fl/+* intercrosses, hence all mice were littermates. KspCre-negative animals were used as controls. *Pkd1 fl/fl*[19] and *NesCre*[20] animals were obtained from JAX Laboratories.

### Transcriptome and gene set enrichment analysis

Control (*Raptor fl/fl* or *Kif3a fl/fl* mice), control$^{\Delta RAP}$ (*Raptor fl/fl*KspCre*), CyKD (*Kif3a fl/fl*KspCre*), and CyKD$^{\Delta RAP}$ (*Raptor fl/fl*Kif3a fl/fl*KspCre*) animals were sacrificed at day 1, week 1 (day 7), week 2 (day 14), and week 4 (day 28). Kidneys were split in half and immediately snap frozen in liquid nitrogen. RNA was purified using standard procedures and analyzed using Affymetrix Mouse Genome 430 2.0 gene chips. Raw data were obtained by standard array hybridization techniques and normalized via the Single Channel Array Normalization algorithm,[21] mapping the probes to the custom chip definition file from the BrainArray resources in version 18 (http://brainarray.mbni.med.umich.edu/Brainarray/Database/CustomCDF/). Pathway analysis was performed using the generally applicable gene set enrichment analysis(GSEA), which determines whether a set of genes is systematically upregulated or downregulated as a whole, albeit individual genes need not be significantly regulated.[22] Raw GSEA *P* values were corrected using the false discovery rate.

We used the ConsensusPathDB information for gene set definitions, containing ≈4000 pathways compiled from different databases.[23]

To identify putative upstream regulators of differentially regulated pathways, we used a regulator-pathway correlation algorithm called transcriptional regulatory associations in pathways (TRAP), consisting of 431 canonical pathways in conjunction with their transcriptional regulators. The canonical pathways were extracted from the MSigDB

(version 3.0) "C2:canonical pathways," and the respective regulators were inferred from the mutual information of pathway-gene regulation in >3000 microarray profiles.[24] To assess the relative importance of regulators concerning significant pathways ($P < 0.05$), we computed the gain in degree centrality (DC) of each regulator from the difference in DC between subnetworks consisting of differentially regulated pathways (as calculated by GSEA) and associated regulators and the full network.[12] The directed mTOR network was compiled from GeneMANIA, a real-time multiple association integration algorithm for predicting gene function.[25,26]

### Morphologic analysis

Mouse kidneys were perfusion fixed in 4% phosphate-buffered paraformaldehyde, embedded in paraffin, and further processed for periodic acid–Schiff or immunofluorescence staining. Images were acquired using an Axioplan microscope equipped with a digital camera, an Axio Observer Z1 microscope (both from Carl Zeiss Microimaging GmbH), or a Thunder Imager (Leica Microsystems).

### Western blot analysis

Kidneys were glass-glass homogenized in lysis buffer for 2 minutes (modified radioimmunoprecipitation a buffer containing: 50 mM Tris/HCl, pH 7,5, 1 mM ethyleneglycol-bis-(β-aminoethylether)-*N,N,N′,N′*-tetraacetic acid, 1 mM ethylenediamine tetraacetic acid, 1% [w/v] Triton X-100, 0.1 % [w/v] sodium dodecylsulfate, 50 mM NaF, 150 mM NaCl, 0.5% [w/v] Na-deoxycholate, 0.1% [v/v] 2-mercaptoethanol, 1 mM Na-orthovanadate, Roche Ultra complete proteinase inhibitor cocktail, and Roche Phospho-STOPP, as indicated by the manufacturer [Roche] and double-distilled water at final volume; 15 µl lysis buffer per 1 mg of tissue was used). Samples were heated after the addition of 2× Laemmli buffer (including 100 mM dithiothreitol) at 42 °C for 30 minutes. Western blots were densitometrically analyzed using LabImage software (Labimage Software).

A list of primary and secondary antibodies used is provided in the Supplementary Methods.

### Magnetic resonance imaging measurement of renal volume

Magnetic resonance imaging experiments were performed on a 9.4-T (400-MHz) horizontal magnet (Bruker Biospin). A quadrature birdcage coil (Bruker Biospin) with an inner diameter of 38 mm was used. Mice were anesthetized with isoflurane and monitored with respect to breathing and heart rate using electrocardiography to ensure that they remained at a constant level.

### Lenti-paired clustered regularly interspaced short palindromic repeats/Cas9 transduction and cyst formation from *PKD1*$^{-/-}$ tubuloids

To isolate cells for tubuloid culture and perform PKD1 gene editing in the tubuloids, we used kidney explants of patients undergoing nephrectomy. The study was approved by the Ethical Board of the Rheinisch-Westfaelische Technische Hochschule (RWTH) Aachen University, Medical Faculty (decision EK016/17), and performed according to the Declaration of Helsinki. Informed consent was given by all patients. CD24$^{+}$ adult human kidney tubuloids were established as recently described.[27] The cysts from PKD1$^{-/-}$ tubuloids were treated with 10, 25, and 50 nM of rapamycin or palbociclib for 72 hours. Equal volume of dimethylsulfoxide and sterile water in the organoid growth medium was used as negative control.

### Real-time reverse transcription–quantitative polymerase chain reaction

Total RNA was isolated from *PKD1*$^{-/-}$ tubuloids and used for reverse transcription–quantitative polymerase chain reaction to quantify *CDK4*, *CDK6*, and *cyclin D1* mRNA expression. Briefly, 250 ng of total RNA was used to synthesize cDNA via SuperScript III First-Strand Synthesis System (18080051, Thermo Fisher Scientific), according to the manufacturer's protocol. Reverse transcription–quantitative polymerase chain reaction was performed in quadruplicate with 1:10 dilution of cDNA, 300 nM primers, and iTAQ SYBR Green Supermix (172-524, Bio-Rad) using CFX Connect Real-time PCR Detection System (Bio-Rad).

### Human kidney organoids from induced pluripotent stem cells

Induced pluripotent stem cell lines used were *PKD1*$^{-/-}$ Q3838X (exon 41 mutant, gRNA CCTGCAGCTGCACAACTGGC) and *PKD2*$^{-/-}$ R872X (exon 14 mutant, gRNA TGGAGCGAGCCAAACTGAAG), both derived from the WTC-11 cell line (Coriell GM25256) using BIG-TREE cytosine base editing plasmids, as described in a parallel publication.[28] Organoids were differentiated as described.[29] To assess toxicity and viability, organoids were manually microdissected on day 21 after cell plating and placed in suspension until day 30. Using wide-bore p200 tips set to a volume of 75 µl, cystic organoids were transferred into 96-well low attachment plates (1 organoid/well). Palbociclib (0.3 µM; SelleckChem, S1116) and everolimus (0.1 µM; SelleckChem, S1120) were diluted in serial dilutions to 4× concentration, and 25 µl of the drugs was added to each well to bring the final volume to 100 µl/well. Medium was changed every other day by removing 50 µl of medium, replacing with fresh 25 µl of medium and fresh 25 µl of compound. Imaging was done on days 0, 1, 3, 7, and 14. On day 14 (end point), a live/dead test was performed.

### Statistical analysis

Data are expressed as mean ± SEM. Statistical comparisons were performed using the GraphPad Prism Software Package 6 (GraphPad Software Inc.) with 2-tailed Student *t* test or analysis of variance, including respective corrections where indicated. Differences with *P* values $< 0.05$ were considered significant.

## RESULTS

mTORC1 activity was genetically eliminated in distal tubular epithelial cells, using *Ksp*-driven *Cre* expression combined with conditional *Raptor* alleles ($^{\Delta Rap}$, Supplementary Figure S1A–H′).

Cyst formation and progressive cystic kidney disease (CyKD) were triggered by concurrent ablation of ciliogenesis using conditional *Kif3a* alleles, generating the CyKD$^{\Delta Rap}$ mouse strain (Figure 1a). Ciliogenesis was equally disrupted in CyKD and CyKD$^{\Delta Rap}$ mice, as indicated by the equal number of cilia at the age of 2 weeks (Supplementary Figure S2A–C). CyKD mice with normal mTORC1 activity rapidly developed renal cysts that became detectable by magnetic resonance imaging 2 weeks after birth. They completely replaced the normal renal parenchyma by 6 weeks (Figure 1b). All CyKD mice died before 12 weeks of age, with a median survival of 7.3 weeks (Figure 1c). Concurrently, simultaneous deletion of *Raptor* dramatically slowed the development of renal cysts during the first 4 weeks of observation in CyKD$^{\Delta Rap}$ mice. Although no cysts were detectable by magnetic resonance imaging 2 weeks after birth, few cysts appeared at 4 weeks, and even at 6 weeks the renal parenchyma remained discernable (Figure 1b). Strikingly, the median survival of CyKD$^{\Delta Rap}$ mice was increased >3 times and notably, the removal of just 1 *Raptor* allele improved median survival by 33% (Figure 1c). The survival benefit was accompanied by a reduction in total kidney volume and delay in renal impairment in CyKD$^{\Delta Rap}$ mice compared with either CyKD mice or CyKD$^{wt/\Delta Rap}$ (Figure 1c). Nevertheless, despite the initial delay, CyKD$^{\Delta Rap}$ animals progressively developed cysts after 6 weeks and ultimately succumbed to renal failure (Figure 1c). This raises questions about the underlying mechanism(s) of cyst formation in mTORC1-deficient tubular cells.

To gain insight into both mTORC1-dependent and mTORC1-independent cystogenesis, we performed a large-scale transcriptome analysis using microarray. Whole-genome Affymetrix Mouse 430 2.0 microarrays were obtained from control, control$^{\Delta Rap}$, CyKD, and CyKD$^{\Delta Rap}$ mice at day 1 and at 1, 2, and 4 weeks of age ($n \geq 7$ per condition and time point with a total of 142 individual gene profiles). We performed a principal component analysis, which indicated that all samples clustered according to their developmental stage from day 1 to week 4, with the most notable separation according to genotype at week 4 (Supplementary Figure S3). Using a GSEA with a curated subset of pathways from the ConsensusPathDB, we found a marked upregulation of the cell cycle in CyKD and inflammation-related processes in CyKD$^{\Delta Rap}$ (Supplementary Table 1) after only 1 week. However, the most substantial increase in gene function from 12 to 405 common pathways for CyKD$^{\Delta Rap}$ and CyKD was evident between 2 and 4 weeks (Supplementary Figure S4A). The comparative analysis of the top 50 shared pathways between CyKD and CyKD$^{\Delta Rap}$ yielded a progressive upregulation of mitogen-activated protein kinase, mTORC2, and AKT signaling pathways and their respective downstream targets in mice lacking mTORC1 activity, suggesting that the loss of mTORC1 is partially replaced by other growth-promoting kinase cascades, including phosphatidylinositol-3′-kinase/AKT and extracellular signal-regulated kinase (Supplementary Figures S4B and S5A and B).

Acknowledging that CyKD mice do not represent an orthologous model of human cystic kidney disease, we compared our findings with the results of an extensive transcriptomic analysis using a conditional *Pkd1* allele.[30] We found a strong correlation between the gene expression in *Pkd1* knock-down mice on day 14 and CyKD mice at weeks 2 and 4, indicating that similar signaling processes lead to cyst manifestation and enlargement in both models (Supplementary Figure S6A). Especially the Gene Ontology terms for cell division/cell cycle, cytoskeleton organization, and chromosome segregation were commonly upregulated, whereas several metabolic signaling pathways were downregulated in both models, underlining the similarity of procystic pathways (Supplementary Figure S6B).

On the basis of the apparent differences in gene expression between 2 and 4 weeks CyKD and CyKD$^{\Delta Rap}$ mice, we aimed to identify key regulators of cyst-promoting pathways, using the transcriptional regulatory associations in pathways (TRAP) network inference algorithm.[24] In this algorithm, regulator-pathway associations are derived from transcriptional coregulation in >3000 individual microarray experiments with transcription factor–coding genes taken from the Riken Transcription Factor Database and Regulator Pathways.[31] Figure 2a depicts the networks of the most significantly enhanced pathways connected through their associated regulators for CyKD$^{\Delta Rap}$ and CyKD at 2 and 4 weeks ($P < 0.05$). A random walk clustering indicated a strong network modularity corresponding to distinctly augmented biological pathways. Strikingly, at 2 weeks, the subnetworks of innate immune response (subnetwork I) and cell cycle (subnetwork II) were highly differentially regulated between CyKD$^{\Delta Rap}$ and CyKD, likely representing the pathways that are responsible for the delay in cyst progression of mTORC1-deficient mice (mTORC1-dependent cyst-promoting factors).

Unexpectedly, at 4 weeks, similarities between CyKD$^{\Delta Rap}$ and CyKD prevailed, with a common upregulation of cell cycle/DNA replication, mitogen-activated protein kinase signaling, and extracellular matrix interactions compared with control animals (Figure 2a). These pathways represent common mTOR-independent cyst-promoting factors that likely explain the recurrence of cyst growth at this stage in CyKD$^{\Delta Rap}$ mice. Histologic assessment of proliferation in CyKD and CyKD$^{\Delta Rap}$ mice using KI67 protein did not show a difference at 4 weeks in the interstitium, whereas proliferation in cyst lining epithelial cells was reduced in CyKD$^{\Delta Rap}$ mice (Supplementary Figure S7).

We next ranked the regulators within each network based on their gain in DC. DC is a standard measure for the relative importance of a node in a network as determined by the respective number and strength of connections. We calculated the gain as the DC ratio of the GSEA subnetworks and the complete TRAP network; a high gain is indicative of the importance of a regulator due to a specific pathway enrichment (Figure 2b).[24] Calculating the DC for the 2 subnetworks'

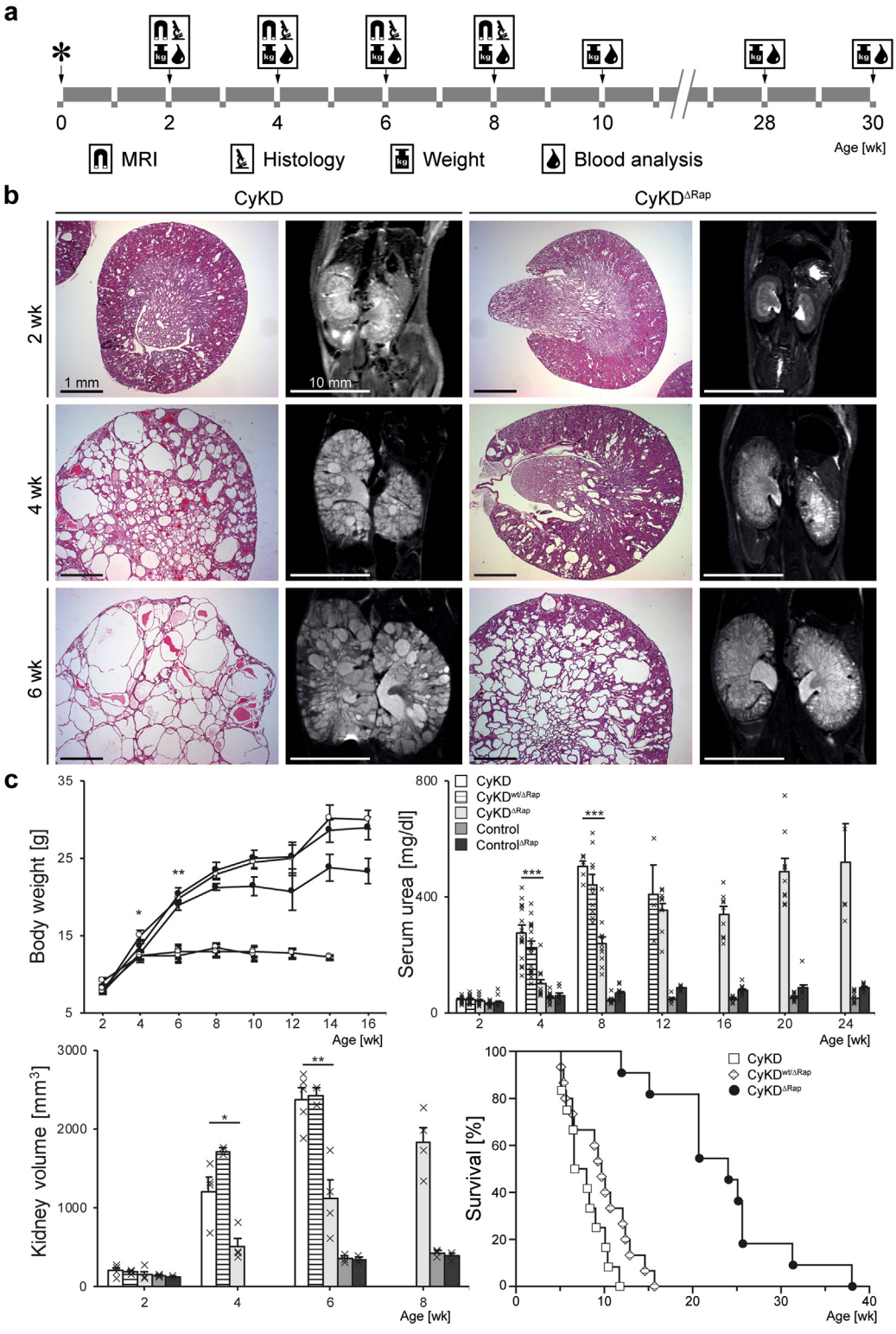


**Figure 1 | Tubule-specific elimination of mammalian target of rapamycin complex 1 activity triples the life span of cilia-deficient mice.** (**a**) Magnetic resonance imaging (MRI), histology, weight, and blood analysis were obtained from the 5 mouse strains up to 30 weeks of age. (**b**) Histology and MRIs demonstrate a striking delay in cyst formation in cystic kidney disease (CyKD)$^{\Delta Rap}$ mice at 2 and 4 weeks compared with Raptor-containing CyKD mice. Even at 6 weeks of age, the cortex of CyKD$^{\Delta Rap}$ kidneys remains largely preserved. (**c**) Body weight rapidly declined in CyKD mice and was accompanied by a rapid increase in serum urea, kidney volume, and a median survival of only 7.3 weeks. In contrast, these parameters remained relatively stable in CyKD$^{\Delta Rap}$ mice over the first 6 weeks, resulting in a median survival of 24.0 weeks. The number of animals in each group and detailed statistics are listed in Supplementary Table Figure S1. To optimize viewing of this image, please see the online version of this article at www.kidney-international.org.

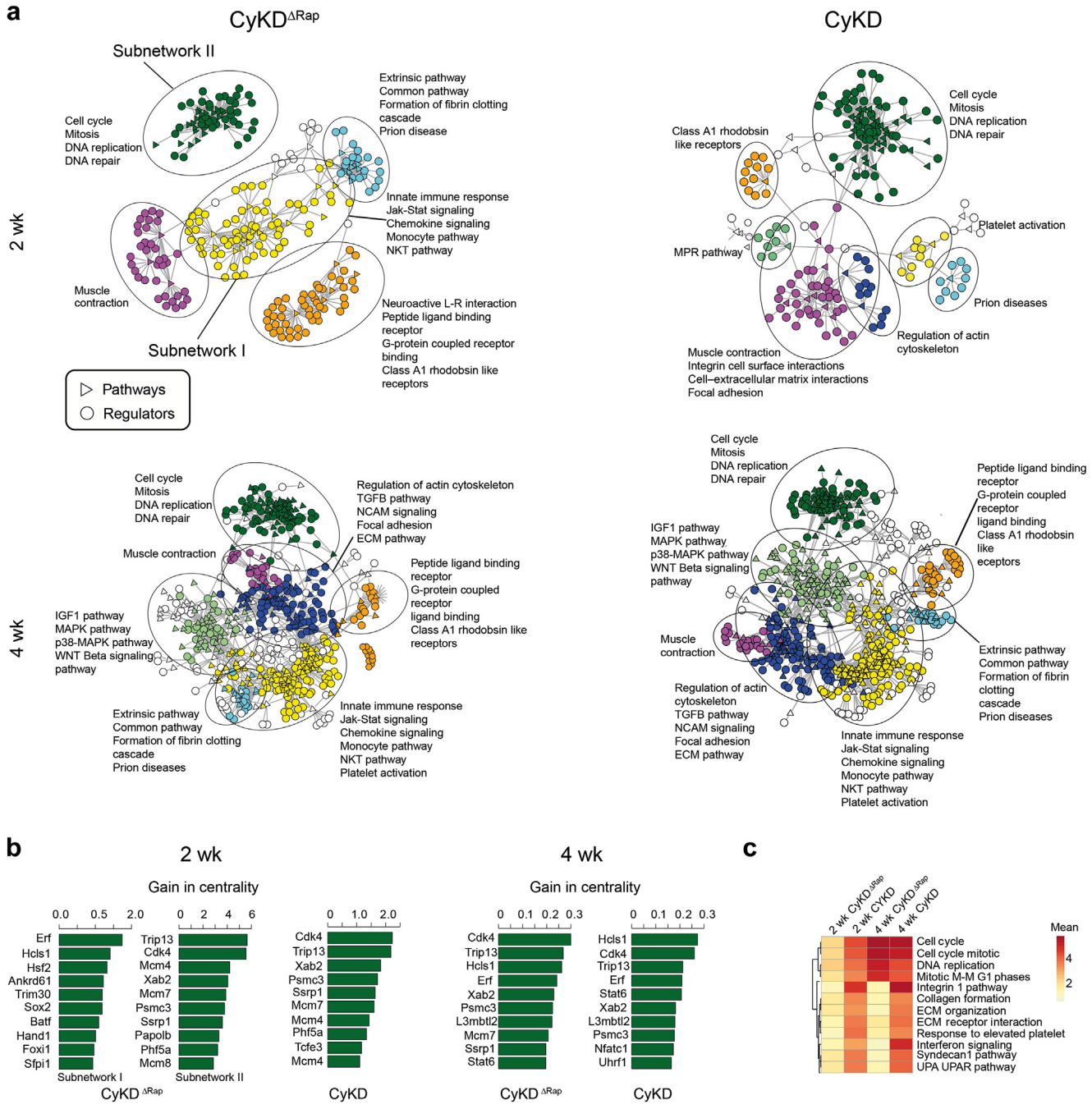


**Figure 2 | The elimination of mammalian target of rapamycin complex 1 activity is rapidly compensated by other growth-promoting pathways.** (**a**) Regulator-pathway networks constructed from transcriptional regulatory associations in pathways (TRAP). Triangles depict the significantly upregulated pathways (gene set enrichment analysis [GSEA] false discovery rate corrected $P < 0.05$) together with their associated regulators (circles) for cystic kidney disease (CyKD)$^{\Delta RAP}$ and CyKD at 2 and 4 weeks relative to wild-type controls. A random walk algorithm clustered the networks into different submodules, demonstrating a significant difference between CyKD$^{\Delta RAP}$ and CyKD at 2 weeks. Although both CyKD$^{\Delta RAP}$ and CyKD contain a cluster cell cycle process, the former encompasses immune response in a disjoint subnetwork. At 4 weeks, CyKD$^{\Delta RAP}$ and CyKD have similar pathways. (**b**) The top 10 transcriptional regulators putatively control the significant pathways in the GSEA-enriched TRAP subnetworks from (**a**). Regulators were ranked according to their gain in degree centrality (DC), which denotes the ratio of the weighted edges per regulator for each fully connected GSEA-enriched subnetwork with respect to all regulator-pathway connections of the entire TRAP network. Note the separate DC analyses for the 2 subnetworks in CyKD$^{\Delta RAP}$ at 2 weeks. In both conditions, *Erf/Hcls* and *Trip13/Cdk4* are predicted as the most dominating immune responses and cell cycle processes, respectively. (**c**) The heat map illustrates the quantitative change of the mean expression of upregulated cell cycle pathways according to GSEA. The figure demonstrates an early and strong upregulation of these pathways in CyKD compared with CyKD$^{\Delta RAP}$. A striking upregulation in cell cycle pathways occurred in CyKD$^{\Delta RAP}$ beyond 2 weeks. ECM, extracellular matrix.

innate immune response and cell cycle in CyKD$^{\Delta Rap}$ mice showed that the immune response regulator *Hcls1* (*hematopoietic cell-specific Lyn substrate 1*), as well as the cell cycle regulators *Trip13* (thyroid hormone receptor interacting protein 13) and *Cdk4* (cyclin-dependent kinase 4), had the highest gains in each network and ranked highest at 4 weeks. In CyKD, the top DC regulators were almost exclusively related to cell cycle regulation at both time points. Recognizing the qualitative dominance of cell cycle and immune response pathways both at 2 and 4 weeks, we analyzed the quantitative dynamics of these pathways and confirmed a time-dependent difference for cell cycle pathways between the 2 mouse models. As expected, cell cycle pathways were earlier and stronger upregulated in CyKD compared with CyKD$^{\Delta Rap}$, underlining that the elimination of mTORC1 (*Raptor*) transiently caused transcriptional differences. Strikingly, at 4 weeks, the transcriptional profiles and signaling pathways became almost indistinguishable between CyKD and CyKD$^{\Delta Rap}$ mice, coinciding with the delayed appearance of cysts in CyKD$^{\Delta Rap}$ mice (Figure 2c). These findings demonstrate that other signaling cascades rapidly replace the loss of mTORC1.

We corroborated these findings by analyzing CD3 and CD68 infiltrating immune cells in the different mouse models. At 2 weeks, there was an insignificant trend for higher CD68 cell numbers in CyKD versus CyKD$^{\Delta Rap}$ animals (Figure 3a, b, and i). At 4 weeks, the CD68 cell numbers were higher in CyKD versus CyKD$^{\Delta Rap}$ animals (Figure 3 c, d, and i). At both 2 and 4 weeks, the number of CD3-positive cells were similar in CyKD$^{\Delta Rap}$ and CyKD (Figure 3e–i). Our analysis of immune cell infiltration is supported by a cell type enrichment analysis of the transcriptome data using xCell (Supplementary Figure S8A).[32] The normalized enrichment score shows a general trend toward a higher immune and microenvironment score with cyst progression, with a steep incline between 2 and 4 weeks and the strongest enrichment in CyKD mice (Supplementary Figure S8A). The immune score correlates with an increase in macrophages, monocytes, and dendritic cells. Cyst progression also leads to a decrease in fibroblasts and endothelial cells, whereas the relative abundance of epithelial cells is increased.

To elucidate the downstream transcriptional targets of the identified regulators driving cell cycle progression, we focused on signaling pathway-related gene sets in CyKD$^{\Delta Rap}$ and CyKD at 2 and 4 weeks. Extracting all gene sets from the ConsensusPathDB that contained the terms signaling, cascade, or the proprietary names of previously identified pathways yielded a weak regulatory overlap between CyKD and CyKD$^{\Delta Rap}$ at week 2 (Supplementary Figures S8–S11). At 4 weeks, several upstream and downstream pathways of mTOR were jointly regulated in both genotypes. In particular, this applied to *c-Myc*, *Jak/Stat*, *p38/Jnk*, *Erk*, *Rac*, *Plc/Pkc*, and *Tgfβ* signaling, which all showed slightly stronger mean activity in CyKD compared with CyKD$^{\Delta Rap}$ animals (Supplementary Figures S8–S11).

We decided to further explore the role of *Cdk4* as a central driver of cyst formation, bypassing the lack of mTORC1. Immunofluorescence staining of renal sections of CyKD$^{\Delta Rap}$ animals at 4 weeks showed a strong expression of Cdk4 protein in cyst-lining tubular epithelial cells, whereas non-affected tubular and interstitial cells did not show a prominent signal (Figure 4a). Cdk4 protein expression, assessed by Western blot analysis, was 30% higher in CyKD than in CyKD$^{\Delta Rap}$ animals at 2 weeks, whereas CDK4 abundance was reversed at 4 weeks, being increased by 55% in CyKD$^{\Delta Rap}$ compared with CyKD mice (Supplementary Figure S12A and B). This change in protein expression is additionally reinforced by an increased expression of CDK4/6 inhibitors (namely, Cdkn1a, Cdkn1b, Cdkn2b, and Cdkn2d) together with the Cdkn upstream activator Tfap2a in CyKD compared with CyKD$^{\Delta Rap}$ mice (Supplementary Figure S12E and F). The only exception is Cdkn1c, which is significantly downregulated in both conditions after 4 weeks, but more significantly in CyKD mice. The induction of Cdk4/6 inhibitors could potentially stem from transforming growth factor-β signaling through the Smad/2/3/4 heterotrimer. The latter pathway shows the strongest upregulation between CyKD$^{\Delta Rap}$ and CyKD mice at 4 weeks and occurs in the context of fibrosis in ADPKD.[33] Similarly, there was a higher TRIP13 expression in CyKD mice at 2 weeks, whereas TRIP13 levels were similar in CyKD$^{\Delta Rap}$ and CyKD animals at 4 weeks (Supplementary Figure S12A and C). TRIP13 may also represent an important driver of cyst formation because this AAA-ATPase can transform nonmalignant cells and promotes treatment resistance of tumors through enhanced DNA repair.[34]

Palbociclib is a US Food and Drug Administration–approved CDK4/6 inhibitor.[35,36] To apply our findings to ADPKD, we treated 2-week-old CyKD and CyKD$^{\Delta Rap}$ animals for 4 weeks with 150 mg/kg palbociclib. At 6 weeks of age, we observed an mTOR-independent reduction in 2 kidney weight/body weight in both CyKD and CyKD$^{\Delta Rap}$ (Figure 4b). There was also a considerable improvement in kidney function in both CyKD and CyKD$^{\Delta Rap}$ mice (Figure 4b). Interestingly, senescence-associated secretory phenotype gene set taken from the REACTOME Database showed a relative decrease in activity over time for the mTOR knockdown animals but increased after 4 weeks for the CyKD mice. This is in line with an increased expression of interleukin-6, Stat3, Jun, Fos, Rela, and Nfkb1, but also the CDK4 inhibitors Cdkn1a, Cdkn2a, and Cdkn2b and correlates with the increased immune cell and inflammation signature from the xCell analysis (Supplementary Figures S12 and S13).

To extend our findings to a mouse model of human ADPKD, we used Pkd$^{1tm2Ggg}$;Tg(Nes-cre)$^{1Kln}$ mice, a developmental model of *Pkd1* inactivation.[13] Intriguingly, we found a 30% upregulation of Cdk4 protein levels in knockout compared with control animals and observed a 50% reduction in 2 kidney weight/body weight ratio in animals treated with palbociclib for 6 weeks (Figure 4c). Given the systemic application of palbociclib, we could detect a reduction in CD3- and CD68-positive cells in palbociclib versus untreated

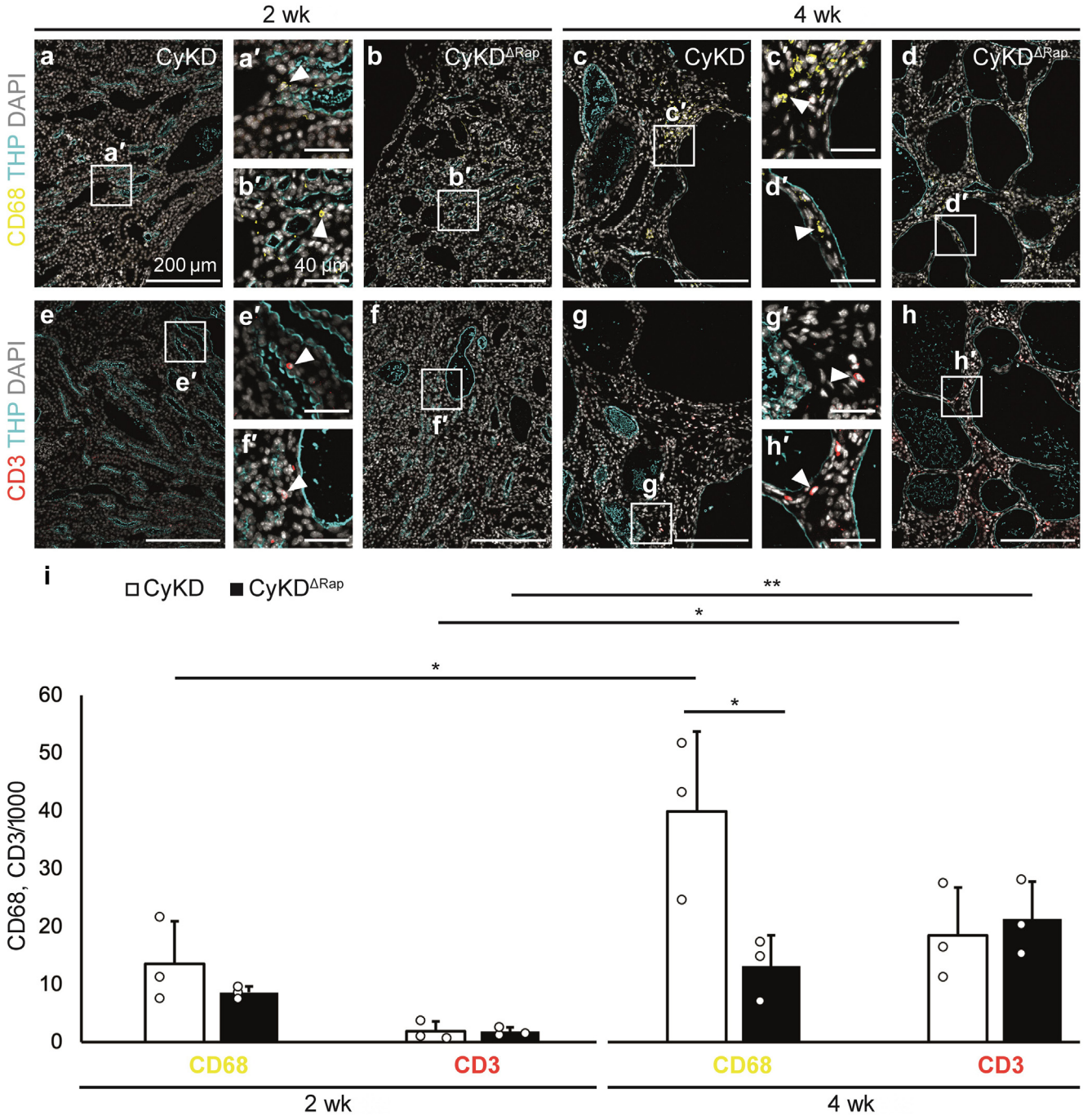


**Figure 3 | Assessment of CD3 and CD68 infiltrating immune cells.** We can show that at 2 weeks there is a trend for more CD68- than CD3-positive cells in (**a** [**a′**, inset], **e** [**e′**, inset]) cystic kidney disease (CyKD) mice ($P = 0{,}054$), whereas this is significant for (**b** [**b′**, inset], **f** [**f′**, inset]) CyKD$^{\Delta RAP}$ ($P = 0.007$). At 4 weeks, there is again a trend for more CD68 than CD3 cells in (**c** [**c′**, inset], **g** [**g′**, inset]) CyKD mice, whereas cell numbers are not different in (**d** [**d′**, inset], **h** [**h′**, inset]) CyKD$^{\Delta RAP}$. (**c** [**c′**, inset], **d** [**d′**, inset]) However, at 4 weeks, macrophage infiltration was found to be higher in CyKD versus CyKD$^{\Delta RAP}$ ($P < 0.05$). (**i**) CD68 and CD3 cells per 1000 nuclei for the aforementioned mice and time points. DAPI, 4′,6-diamidino-2-phenylindole; THP, Tamm–Horsfall protein. To optimize viewing of this image, please see the online version of this article at www.kidney-international.org.

animals (Figure 5a–f). In addition, there was a robust trend of reduced proliferation within the kidneys overall and especially within the cyst-lining epithelium (Figure 5g–i).

To corroborate whether our findings in murine models of PKD can be transferred to human models of PKD, we investigated the effect of mTOR inhibitors and palbociclib in human tubuloids and organoids. In human *PKD1*$^{-/-}$ tubuloids,[27] both rapamycin (10 nM) and palbociclib (10 nM) could inhibit cyst growth by ≈50% compared with placebo-treated controls (Figure 6a–d). Combination of the 2

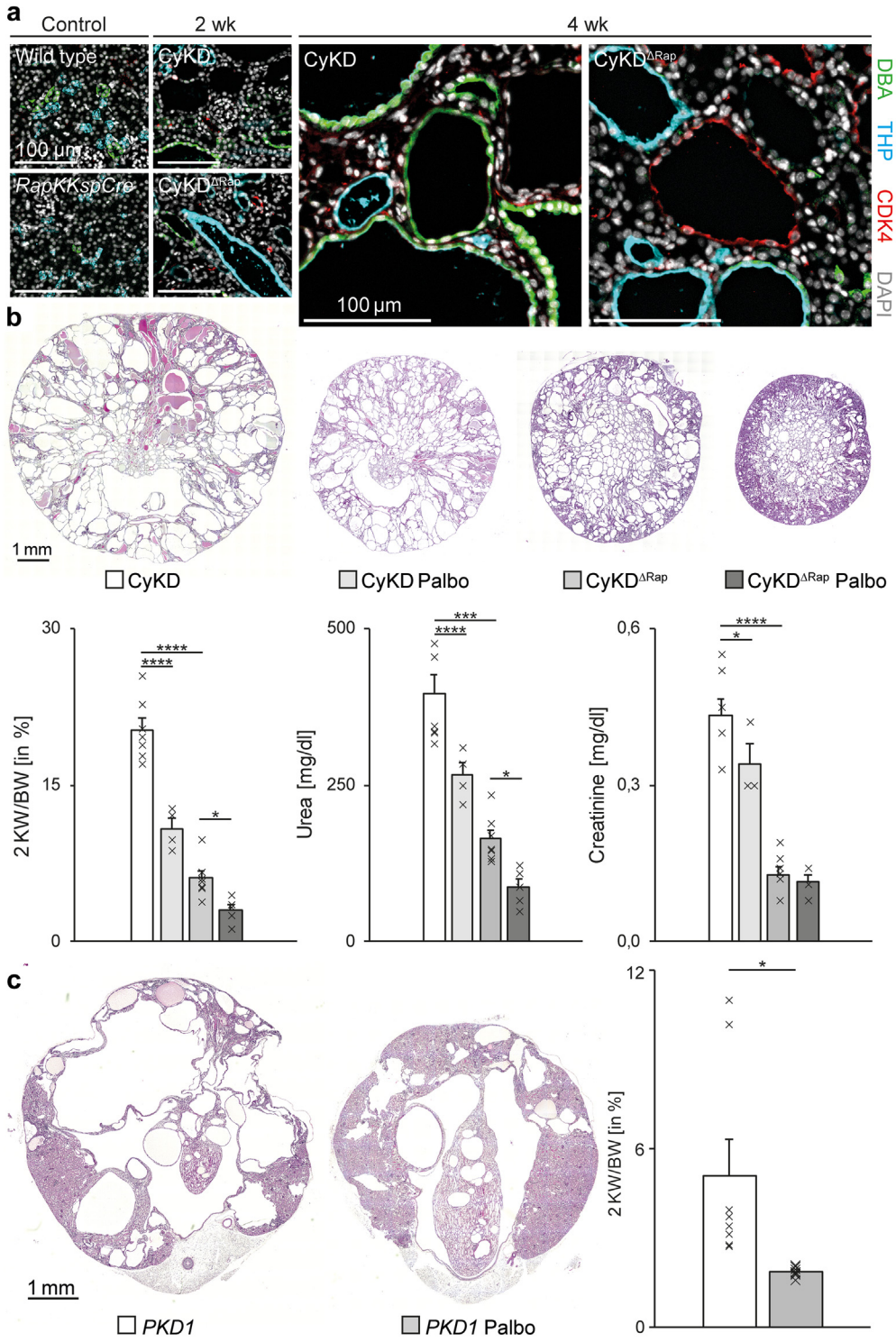


**Figure 4 | Inhibition of cyclin-dependent kinase 4/6 (CDK4/6) reduces kidney growth and substantially improves kidney function.** (**a**) In 4-week-old cystic kidney disease (CyKD)$^{\Delta RAP}$ mice, CDK4 is predominantly expressed in the cyst-lining epithelium, whereas tubules in nonaffected areas only show slight immunoreactivity. (**b**) Histologic cross-sections close to the hilus in CyKD and CyKD$^{\Delta RAP}$ animals, treated with either palbociclib (Palbo; 150 mg/kg orally) or placebo, show a significant size and cyst reduction in all animals treated with palbociclib. The effect was particularly noticeable in CyKD$^{\Delta RAP}$ mice. The efficacy of palbociclib was underlined by a striking reduction in the 2 kidney weight (KW)/body weight (BW) ratio in treated animals. Treatment with palbociclib improved the renal architecture and, most importantly, kidney function, which was most evident regarding the reduction of serum urea values. Serum creatinine values only improved in CyKD animals but not in CyKD$^{\Delta RAP}$ mice, most likely due to the virtually normal values in these animals. (**c**) Similarly to CyKD and CyKD$^{\Delta RAP}$ animals, cyst size and number were reduced in Pkd1 animals. This led to a significant reduction of 2KW/BW.DAPI, 4′,6-diamidino-2-phenylindole; DBA, Dolichos biflorus agglutinin; THP, Tamm–Horsfall protein. To optimize viewing of this image, please see the online version of this article at www.kidney-international.org.

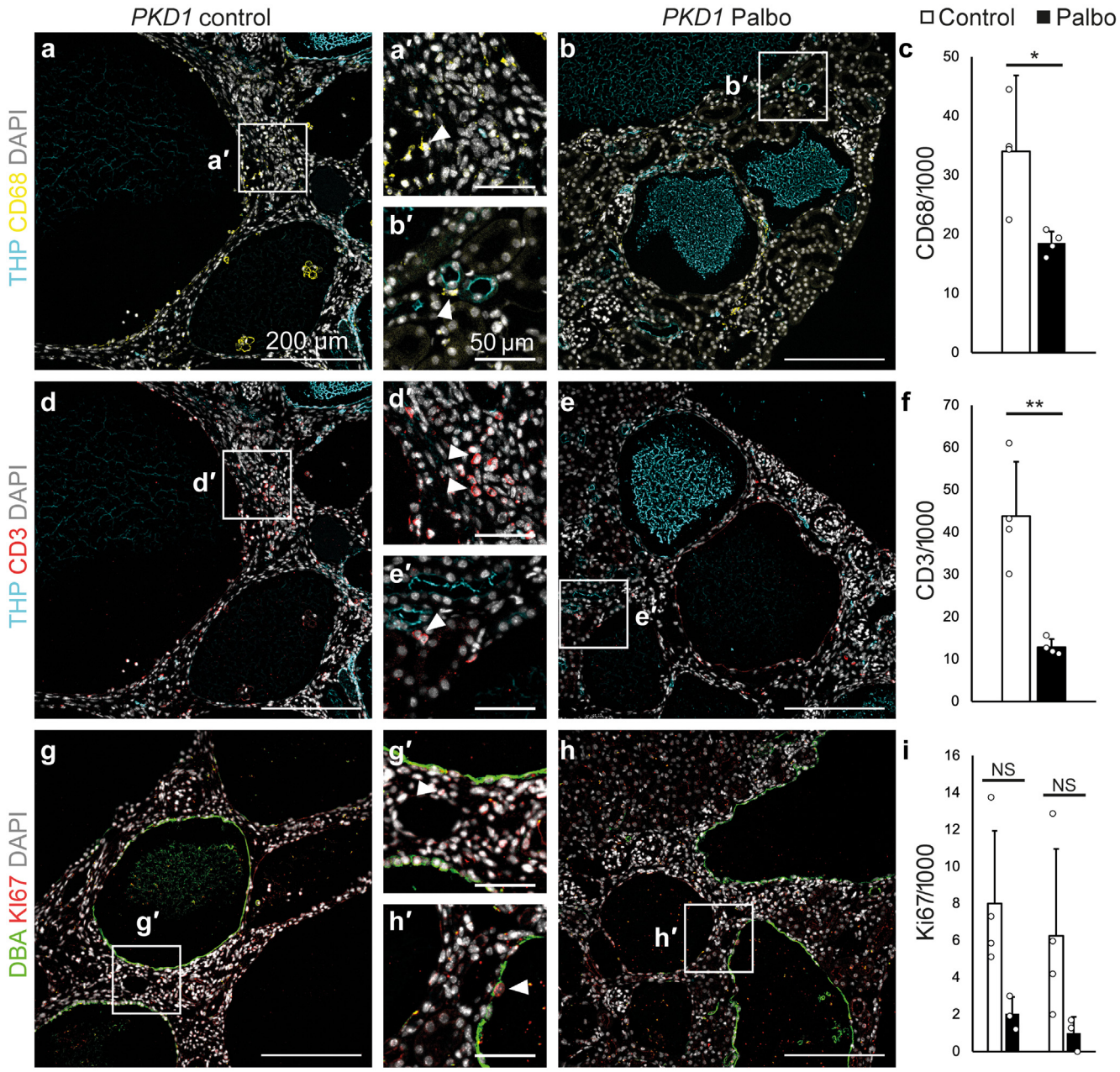


**Figure 5 | Palbociclib (Palbo) reduces immune cell infiltration and proliferation in cyst-lining epithelial cells.** Both T cells and macrophages play a role in regulation of cyst growth in autosomal dominant polycystic kidney disease. We focused our analysis of inflammation on these 2 cell types using immunofluorescent staining for (**a** [**a′**, inset], **b** [**b′**, inset]) CD68 and (**d** [**d′**, inset], **e** [**e′**, inset]) CD3 and quantified immune cell infiltration per 10,000 nuclei. (**c,f**) We found that CD68-positive macrophage infiltration tended to decrease from 34/1000 nuclei to 18.5 in the palbociclib group ($P = 0.1$). T-cell infiltration was reduced from 43.8 T cells/1000 nuclei to 12.8 T cells/1000 nuclei ($P = 0.003$) in the palbociclib group. Proliferation (**g** [**g′**, inset], **h** [**h′**, inset]) was assessed in both cyst epithelial cells and other cells, not stained by Dolichos biflorus agglutinin (DBA) or Tamm–Horsfall protein (THP). Proliferation (**i**) in other cells was found to tend to be decreased from 8 proliferative cells/1000 nuclei to 2 in the palbociclib group ($P = 0.056$), whereas proliferation showed a decreasing trend in cyst epithelial cells from 6.1 in the control group to 0.99 in the palbociclib group ($P = 0.1$). DAPI, 4′,6-diamidino-2-phenylindole; NS, not significant. To optimize viewing of this image, please see the online version of this article at www.kidney-international.org.

inhibitors did reduce cyst growth by ≈60% (Figure 6e), pointing to a potential additive effect of the 2 compounds used. Investigating the expression of *CDKs* in these *PKD1*$^{-/-}$ tubuloids showed a marked upregulation of *CDK4* and *CDK6* but not *CDK1* when rapamycin was used alone, similar to our results in CyKD$^{\Delta Rap}$ mice (Figure 6f–h).

To better pinpoint the potential additive action of combined mTOR and CDK4/6 inhibition, we used human kidney

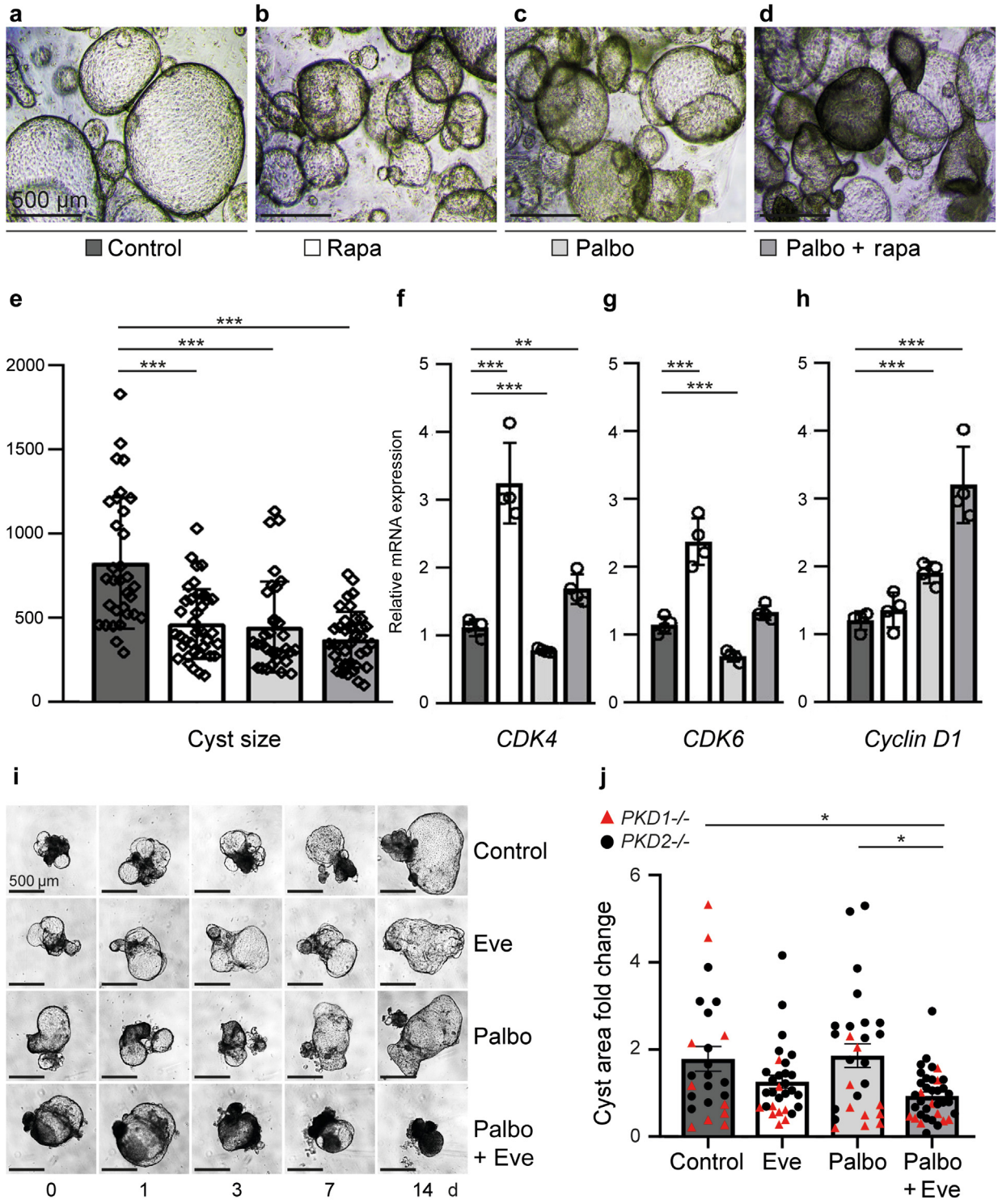


**Figure 6 | Combinatorial treatment reduces cyst growth in human tubuloid and organoid polycystic kidney disease models.** (**a–d**) $CD24^{+}$ adult human kidney tubuloids under indicated treatment regimens. (**e**) Quantification of cyst area; each dot represents a different tubuloid. (**f–h**) Reverse transcription–quantitative polymerase chain reaction of total RNA extracted from tubuloids. Expression of cyclin-dependent kinase 4 (CDK4), CDK6, and cyclin D1 mRNA was normalized by housekeeping gene glyceraldehyde-3-phosphate dehydrogenase and quantified by the ΔΔCt method. (**i**) Representative phase contrast of *PKD1*$^{-/-}$ cystic organoids over time (day 0 = first day of treatment). (**j**) Quantification of cyst area fold change at end point, relative to day 0. Each dot represents a different organoid (mean ± SEM, n > 20 organoids per condition, pooled from 3 independent experiments; of which 2 experiments used *PKD2*$^{-/-}$ organoids [black squares] and 1 experiment used *PKD1*$^{-/-}$ organoids [red triangles]; *$P \leq 0.05$. *P* values for each comparison: control [ctrl] vs. palbociclib [Palbo] 0.9999, ctrl vs. everolimus [Eve] 0.4901, ctrl vs. Palbo + Eve 0.0461, Palbo vs. Eve 0.2986, Palbo vs. Palbo + Eve 0.0164, Eve vs. Palbo + Eve 0.3468). Rapa, rapamycin. To optimize viewing of this image, please see the online version of this article at www.kidney-international.org.

organoids derived from *PKD1*$^{-/-}$ or *PKD2*$^{-/-}$ pluripotent stem cells. These form cysts from kidney tubules, a phenotype that is not observed in isogenic controls.[29,37] We applied this system to assess the capacity of palbociclib, everolimus, or their combination to affect human PKD cyst growth. Organoids were transfered into suspension culture and allowed to initiate cystogenesis, after which treatments were added at doses found to be nontoxic in a preliminary screen (Supplementary Figure S14). Cystic organoids treated with the combination of palbociclib plus everolimus exhibited a significant decrease in cyst growth, compared with control treatments, whereas everolimus or palbociclib alone did not exhibit a significant effect (Figure 6i and j). Live-dead analysis further demonstrated that these treatment conditions were not toxic to the organoids over the time course of the experiment (Supplementary Figure S14). Both human PKD model systems support a combinatorial treatment approach with mTOR and CDK4/6 inhibition in line with our murine data.

## DISCUSSION

Our results have important implications demonstrating that mTORC1 is an important driver of cyst growth and disease progression; mice lacking mTORC1 experience improved kidney function and substantially increased survival rates. Thus, mTORC1 remains an important therapeutic target to curtail cystic kidney disease. However, abrogation of mTORC1 activity alone only transiently slowed cyst growth; other growth-promoting pathways were rapidly activated and bypassed mTORC1 to promote disease progression. Bypass mechanisms, resulting from disinhibiting negative feedback loops, are frequently observed in solid tumors treated with highly specific receptor tyrosine kinase inhibitors,[38] and require combinatorial or sequential drug regimens to maintain efficacy.[39] The latter was successfully demonstrated in the treatment of glioblastoma.[40] Our results indicate that similar therapeutic concepts might be required to treat cystic kidney disease. The combination of *in vivo* experiments and mathematical modeling applied to our microarray-based transcriptome data set identified the (sub-)networks of innate immune response and cell cycle as key networks driving cyst formation.

Using this information, we show that over time increased numbers of especially macrophages in CyKD mice compared with CyKD$^{\Delta Rap}$ animals could potentially contribute to the higher cyst burden in CyKD mice. We could next demonstrate the superior efficacy of a combined Cdk4 and mTORC1 inhibition in a murine model of cystic kidney disease. We further extended this to a human tubuloid PKD model, where we recapitulated upregulation of CDK4/6 with rapamycin monotherapy, whereas in a human organoid PKD model, the application of everolimus and palbociclib proved synergistic compared with monotherapy. CDK4 controls the Rb-regulated $G_1$/S cell-cycle checkpoint. Although CDK4 phosphorylates and inactivates the Rb tumor suppressor to release the E2F transcription factors, initiating transcription of genes required for DNA replication, CDK4/6 inhibitors shift the balance from proliferative toward apoptotic programs.[41,42] Additionally, the CDK4/6 inhibitor reduced immune cell infiltration into cystic kidneys, which could provide another means of slowing down disease progression. The combinatorial treatment not only reduced kidney size in mice and cyst size in organoid models but also approximated the kidney function to wild-type animals.

Our data suggest that bypass signaling, similar to the rapid adaptation observed in response to selective cancer treatment, can drive cyst growth after inhibiting a single key signaling pathway. In addition, it calls for more specific inhibitors to reduce adverse effects and to allow for combinatorial treatments. While demonstrating the crucial role of the $G_1$/S cell cycle regulator CDK4 in promoting cyst formation and disease progression, our findings also explain why short-term inhibition of mTORC1 in ADPKD seems beneficial,[43–45] and underline the need for further treatment concepts in polycystic kidney disease.

## DISCLOSURE

PM has been an employee of Novartis Pharma AG, Basel, Switzerland. TBH has received project-specific grant funding from Pfizer Pharma GmbH and acted as a consultant for Pfizer Pharma in the past. GW has worked as a consultant for Alexion and Otsuka Pharma. BSF is an inventor on patents and/or patent applications related to human kidney organoid differentiation and modeling of PKD in this system (these include "Three-dimensional differentiation of epiblast spheroids into kidney tubular organoids modeling human microphysiology, toxicology, and morphogenesis" [Japan, United States, and Australia], licensed to STEMCELL Technologies; "High-throughput automation of organoids for identifying therapeutic strategies" [PTC patent application pending]; and "Systems and methods for characterizing pathophysiology" [PTC patent application pending]). BSF holds ownership interest in Plurexa LLC. All the other authors declared no competing interests.

## DATA STATEMENT

Microarray data have been deposited at Gene Expression Omnibus (GEO) under the identifier GSE58044. Software, algorithms, animal and organoid models, protocols, and other materials and resources related to the manuscript will be made available on request.

## ACKNOWLEDGMENTS

We thank Betina Kiefer, Charlotte Meyer, Temel Kilic, and Annette Merkle for expert technical assistance. This study was supported as follows: FG was supported by the Deutsche Forschungsgemeinschaft (DFG; German Research Foundation) (CRC 1140, CRC 1192, GR3933/1-1); BD was supported by the DFG (Walter Benjamin Stipendium DU 2449/1-1); HW was supported by CSC (202208080139); TBH was supported by the DFG (CRC1192, HU 1016/8-2, HU 1016/11-1, HU 1016/ 12-1), by the German Federal Ministry of Education and Research (BMBF) (STOP-FSGS-01GM1901C, NephrESA-031L0191E, and UPTAKE- 01EK2105D), and by the H2020-IMI2 consortium BEAt-DKD (115974) this joint undertaking receives support from the European Union's Horizon 2020 research and innovation program and EFPIA and JDRF; BSF was supported by NIH awards R01DK117914, 1R41DK136452, and UH3TR003288, the Lara Nowak-Macklin Research Fund, and a Washington Research Foundation Phase 1 Technology Commercialization Grant; GW was supported by the DFG (KFO201,

CRC 1140, CRC 1453) and the Else-Kröner-Fresenius-Stiftung; FA was supported by the DFG (CRC 1453); VGP was supported by DFG (CRC 1192), by BMBF (eMed consortium "Fibromap"), and by Novo Nordisik Foundation (Young Investigator Award; NNF21OC0066381); MB was supported by the DFG within the CRC1160 (Project ID 256073931-Z02), CRC/TRR167 (Project ID 259373024-Z01), CRC1453 (Project ID 431984000-S1), CRC1479 (Project ID: 441891347- S1), and by the BMBF within the Medical Informatics Funding Scheme - MIRACUM-FKZ 01ZZ1801B; HB was funded by the DFG, under Germany`s Excellence Strategy – EXC 22167-390884018 and the BMBF (Gerontosys II-NephAge); and NS was supported by the DFG (SPP1395 InKomBio). The authors thank the Core Facility AMIRCF (DFG-RIsources N° RI_00052) for support in small animal imaging.

## AUTHOR CONTRIBUTIONS

FG, GW, and TBH conceived the study. HB, NS, PM, and MB provided and performed transcriptomic analysis of microarrays. FG, BD, REG, HW, YX, FA, LS, TC, AT, VP, RK, BSF, and WR performed and analyzed experiments. FG, GW, BSF, HB, MB, and TBH wrote the manuscript, with input and final approval from all authors.

Supplementary material is available online at www.kidney-international.org.

## REFERENCES

1. Torres VE, Harris PC, Pirson Y. Autosomal dominant polycystic kidney disease. *Lancet*. 2007;369:1287–1301.
2. Ong AC, Devuyst O, Knebelmann B, et al. Autosomal dominant polycystic kidney disease: the changing face of clinical management. *Lancet*. 2015;385:1993–2002.
3. Hildebrandt F, Benzing T, Katsanis N. Ciliopathies. *N Engl J Med*. 2011;364:1533–1543.
4. Ibraghimov-Beskrovnaya O, Natoli TA. mTOR signaling in polycystic kidney disease. *Trends Mol Med*. 2011;17:625–633.
5. Shillingford JM, Murcia NS, Larson CH, et al. The mTOR pathway is regulated by polycystin-1, and its inhibition reverses renal cystogenesis in polycystic kidney disease. *Proc Natl Acad Sci U S A*. 2006;103:5466–5471.
6. Qin S, Taglienti M, Nauli SM, et al. Failure to ubiquitinate c-Met leads to hyperactivation of mTOR signaling in a mouse model of autosomal dominant polycystic kidney disease. *J Clin Invest*. 2010;120:3617–3628.
7. Boehlke C, Kotsis F, Patel V, et al. Primary cilia regulate mTORC1 activity and cell size through Lkb1. *Nat Cell Biol*. 2010;12:1115–1122.
8. Grahammer F, Haenisch N, Steinhardt F, et al. mTORC1 maintains renal tubular homeostasis and is essential in response to ischemic stress. *Proc Natl Acad Sci U S A*. 2014;111:E2817–E2826.
9. Grahammer F, Wanner N, Huber TB. mTOR controls kidney epithelia in health and disease. *Nephrol Dial Transplant*. 2014;29(suppl 1):i9–i18.
10. Huber TB, Walz G, Kuehn EW. mTOR and rapamycin in the kidney: signaling and therapeutic implications beyond immunosuppression. *Kidney Int*. 2011;79:502–511.
11. Fantus D, Rogers NM, Grahammer F, et al. Roles of mTOR complexes in the kidney: implications for renal disease and transplantation. *Nat Rev Nephrol*. 2016;12:587–609.
12. Tao Y, Kim J, Schrier RW, et al. Rapamycin markedly slows disease progression in a rat model of polycystic kidney disease. *J Am Soc Nephrol*. 2005;16:46–51.
13. Shillingford JM, Piontek KB, Germino GG, et al. Rapamycin ameliorates PKD resulting from conditional inactivation of Pkd1. *J Am Soc Nephrol*. 2010;21:489–497.
14. Serra AL, Poster D, Kistler AD, et al. Sirolimus and kidney growth in autosomal dominant polycystic kidney disease. *N Engl J Med*. 2010;363:820–829.
15. Walz G, Budde K, Mannaa M, et al. Everolimus in patients with autosomal dominant polycystic kidney disease. *N Engl J Med*. 2010;363:830–840.
16. Bentzinger CF, Romanino K, Cloetta D, et al. Skeletal muscle-specific ablation of raptor, but not of rictor, causes metabolic changes and results in muscle dystrophy. *Cell Metab*. 2008;8:411–424.
17. Shao X, Somlo S, Igarashi P. Epithelial-specific Cre/lox recombination in the developing kidney and genitourinary tract. *J Am Soc Nephrol*. 2002;13:1837–1846.
18. Lin F, Hiesberger T, Cordes K, et al. Kidney-specific inactivation of the KIF3A subunit of kinesin-II inhibits renal ciliogenesis and produces polycystic kidney disease. *Proc Natl Acad Sci U S A*. 2003;100:5286–5291.
19. Piontek KB, Huso DL, Grinberg A, et al. A functional floxed allele of Pkd1 that can be conditionally inactivated *in vivo*. *J Am Soc Nephrol*. 2004;15:3035–3043.
20. Tronche F, Kellendonk C, Kretz O, et al. Disruption of the glucocorticoid receptor gene in the nervous system results in reduced anxiety. *Nat Genet*. 1999;23:99–103.
21. Piccolo SR, Sun Y, Campbell JD, et al. A single-sample microarray normalization method to facilitate personalized-medicine workflows. *Genomics*. 2012;100:337–344.
22. Luo W, Friedman MS, Shedden K, et al. GAGE: generally applicable gene set enrichment for pathway analysis. *BMC Bioinformatics*. 2009;10:161.
23. Kamburov A, Stelzl U, Lehrach H, et al. The ConsensusPathDB interaction database: 2013 update. *Nucleic Acids Res*. 2013;41:D793–D800.
24. Kwong LN, Costello JC, Liu H, et al. Oncogenic NRAS signaling differentially regulates survival and proliferation in melanoma. *Nat Med*. 2012;18:1503–1510.
25. Mostafavi S, Ray D, Warde-Farley D, et al. GeneMANIA: a real-time multiple association network integration algorithm for predicting gene function. *Genome Biol*. 2008;9(suppl 1):S4.
26. Warde-Farley D, Donaldson SL, Comes O, et al. The GeneMANIA prediction server: biological network integration for gene prioritization and predicting gene function. *Nucleic Acids Res*. 2010;38:W214–W220.
27. Xu Y, Kuppe C, Perales-Paton J, et al. Adult human kidney organoids originate from CD24(+) cells and represent an advanced model for adult polycystic kidney disease. *Nat Genet*. 2022;54:1690–1701.
28. Vishy CE, Thomas C, Vincent T, et al. Genetics of cystogenesis in base-edited human organoids reveal therapeutic strategies for polycystic kidney disease. *Cell Stem Cell*. 2024;31:537–553.e5.
29. Freedman BS, Brooks CR, Lam AQ, et al. Modelling kidney disease with CRISPR-mutant kidney organoids derived from human pluripotent epiblast spheroids. *Nat Commun*. 2015;6:8715.
30. Menezes LF, Zhou F, Patterson AD, et al. Network analysis of a Pkd1-mouse model of autosomal dominant polycystic kidney disease identifies HNF4alpha as a disease modifier. *PLoS Genet*. 2012;8:e1003053.
31. Subramanian A, Tamayo P, Mootha VK, et al. Gene set enrichment analysis: a knowledge-based approach for interpreting genome-wide expression profiles. *Proc Natl Acad Sci U S A*. 2005;102:15545–15550.
32. Aran D, Hu Z, Butte AJ. xCell: digitally portraying the tissue cellular heterogeneity landscape. *Genome Biol*. 2017;18:220.
33. Hassane S, Leonhard WN, van der Wal A, et al. Elevated TGFbeta-Smad signalling in experimental Pkd1 models and human patients with polycystic kidney disease. *J Pathol*. 2010;222:21–31.
34. Banerjee R, Russo N, Liu M, et al. TRIP13 promotes error-prone nonhomologous end joining and induces chemoresistance in head and neck cancer. *Nat Commun*. 2014;5:4527.
35. Fry DW, Harvey PJ, Keller PR, et al. Specific inhibition of cyclin-dependent kinase 4/6 by PD 0332991 and associated antitumor activity in human tumor xenografts. *Mol Cancer Ther*. 2004;3:1427–1438.
36. Turner NC, Ro J, Andre F, et al. Palbociclib in hormone-receptor-positive advanced breast cancer. *N Engl J Med*. 2015;373:209–219.
37. Cruz NM, Song X, Czerniecki SM, et al. Organoid cystogenesis reveals a critical role of microenvironment in human polycystic kidney disease. *Nat Mater*. 2017;16:1112–1119.
38. Niederst MJ, Engelman JA. Bypass mechanisms of resistance to receptor tyrosine kinase inhibition in lung cancer. *Sci Signaling*. 2013;6:re6.
39. Crystal AS, Shaw AT, Sequist LV, et al. Patient-derived models of acquired resistance can identify effective drug combinations for cancer. *Science*. 2014;346:1480–1486.
40. Olmez I, Brenneman B, Xiao A, et al. Combined CDK4/6 and mTOR inhibition is synergistic against glioblastoma via multiple mechanisms. *Clin Cancer Res*. 2017;23:6958–6968.
41. Cristofanilli M, Turner NC, Bondarenko I, et al. Fulvestrant plus palbociclib versus fulvestrant plus placebo for treatment of hormone-receptor-positive, HER2-negative metastatic breast cancer that progressed on previous endocrine therapy (PALOMA-3): final analysis of the multicentre, double-blind, phase 3 randomised controlled trial. *Lancet Oncol*. 2016;17:425–439.

42. Verma S, Bartlett CH, Schnell P, et al. Palbociclib in combination with fulvestrant in women with hormone receptor-positive/HER2-negative advanced metastatic breast cancer: detailed safety analysis from a multicenter, randomized, placebo-controlled, phase III study (PALOMA-3). *Oncologist*. 2016;21:1165–1175.
43. Braun WE, Schold JD, Stephany BR, et al. Low-dose rapamycin (sirolimus) effects in autosomal dominant polycystic kidney disease: an open-label randomized controlled pilot study. *Clin J Am Soc Nephrol*. 2014;9:881–888.
44. Soliman A, Zamil S, Lotfy A, et al. Sirolimus produced S-shaped effect on adult polycystic kidneys after 2-year treatment. *Transplant Proc*. 2012;44:2936–2939.
45. Perico N, Antiga L, Caroli A, et al. Sirolimus therapy to halt the progression of ADPKD. *J Am Soc Nephrol*. 2010;21:1031–1040.